Arrest of Flow and Emergence of Activated Processes at the Glass Transition of a Suspension of Particles with Hard Spherelike Interactions

W. van Megen, V. A. Martinez, and G. Bryant

Department of Applied Physics, Royal Melbourne Institute of Technology, Melbourne, Victoria 3000, Australia

(Received 24 November 2008; published 23 April 2009)

By combining aspects of the coherent and self-intermediate scattering functions, we show that the arrest of particle number density fluctuations spreads from the position of the main structure factor peak. We propose that this arrest impairs the system's ability to respond to diffusing momentum currents, leading to an enhanced resistance to flow. From the stretching of the coherent intermediate scattering functions in the glass, we read a manifestation of the undissipated thermal energy—the source of the ergodicity restoring processes that short-circuit the sharp transition to a perfect glass.

DOI: 10.1103/PhysRevLett.102.168301 PACS numbers: 82.70.Dd, 61.20.Ne

We report dynamic light scattering measurements that simultaneously expose the arrest of flow and the emergence of activated processes at the glass transition of a suspension of particles with hard spherelike interactions. Despite numerous studies over the past two decades [1], the process of vitrification, even of systems with simple interactions, remains poorly understood. The question that continues to be posed is, ''What are the mechanisms that cause structural relaxation to slow and resistance to flow to increase so sharply when a liquid is (under)cooled below its normal freezing temperature?'' Interestingly, efforts to answer this question generally ignore one important aspect of the phenomenology—the fact that vitrification is a consequence of the suppression of crystallization. Indeed, one might ask, ''What precisely is it about the kinetic path, that nucleates the crystal phase, that can be frustrated to such an extent that the solid that emerges is amorphous rather than crystalline?''

To address these issues, we combine aspects of the coherent and incoherent (or self-) intermediate scattering functions (ISFs), obtained by dynamic light scattering (DLS). Although both ISFs of hard-sphere suspensions have been measured previously [2–4], recent improvements in experimental procedures make it possible to express the particle number density fluctuations in terms of the single particle displacement.

We concentrate on volume fractions ϕ in the range between the observed first-order freezing transition, at $\phi_f(= 0.494)$, and the glass transition (GT), at $\phi_g(\approx 0.565)$ [5]. A small spread in the particle radii (polydispersity) delays nucleation of the crystalline phase long enough to measure the dynamical properties of the undercooled suspension [6,7].

Particles of average hydrodynamic radius $R = 200$ nm comprise cores of poly-(methylmethacrylate and trifluoroethylacrylate) with a stabilizing coating of poly-12-hydroxystearic acid approximately 10 nm thick that provides the hard spherelike interaction. Suspension in *cis*-decalin provides samples from which multiple scattering of the laser light is negligible [8]. Including 2% (by volume) of silica particles that have the same radius and stabilizing coating as the polymer particles provides samples for which the scattered light has both coherent and incoherent contributions. Temperature variation allows fine-tuning of the relative scattering amplitudes of the two species to the point where coherent scattering, i.e., scattering from the particle number density fluctuations, is optically suppressed and only the incoherent ISF is measured [3]. Further details of the sample preparation and light scattering procedures are published [3,8].

We begin with the Gaussian limit of the incoherent ISF

$$F_s(q, \tau) = \exp[-q^2\langle\Delta r^2(\tau)\rangle/6], \tag{1}$$

where q is the magnitude of the scattering vector and $\langle\Delta r^2(\tau)\rangle$ the particles' mean-squared displacement (MSD) for delay time τ. The coherent ISF can be expressed in an analogous form as follows:

$$F(q, \tau) = \exp[-q^2 w(q, \tau)]. \tag{2}$$

$\langle\Delta r^2(\tau)\rangle$ and the ''width'' function $w(q_m, \tau)$, examples of which are shown in Fig. 1, are merely alternative representations of the ISFs (also shown). We focus on the maximum deviations from diffusive behavior by locating the inflection points, at delay times $\tau_m^{(s)}$ and $\tau_m^{(c)}(q)$, of the double logarithm plots of $\langle\Delta r^2(\tau)\rangle$ and $w(q, \tau)$ versus τ. The deviations are given by the stretching, or non-Fickian, indices

$$c_s = 1 - \min\left[\frac{d\log\langle\Delta r^2(\tau)\rangle}{d\log\tau}\right] \quad \text{and}$$
$$c_c(q) = 1 - \min\left[\frac{d\log w(q, \tau)}{d\log\tau}\right]. \tag{3}$$

At delay times $\tau_m^{(s)}$ and $\tau_m^{(c)}(q)$, the respective ISFs will have constant contributions, from those particles still caged by their neighbors, and fluctuating contributions, from more mobile particles. The former, represented by the nonergodicity factors, do not survive the differentiation

 © 2009 The American Physical Society

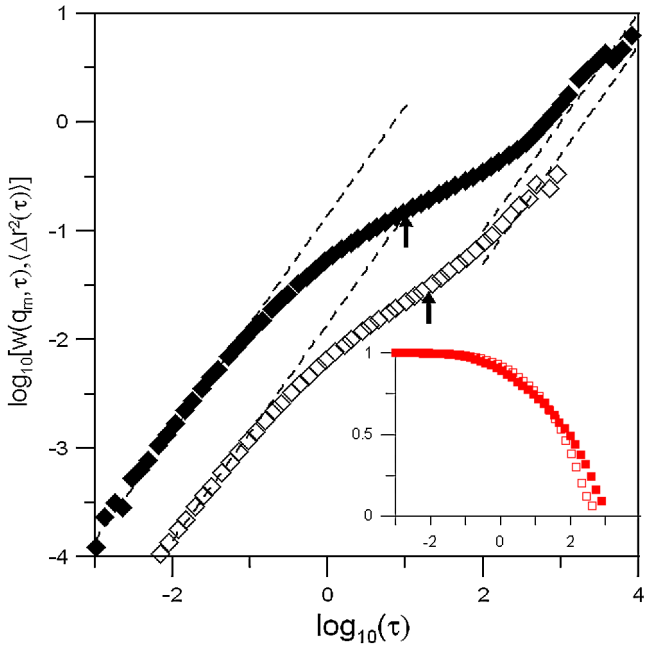

FIG. 1 (color online). MSD $\langle \Delta r^2(\tau) \rangle$ (filled squares) and the width function $w(q_m, \tau)$ (open squares) defined by Eqs. (1) and (2), for the wave vector $q_m R = 3.5$, corresponding to the position of the main structure factor maximum q_m at $\phi = 0.53$. Arrows indicate the inflection points. In this and figures below, distances are expressed in units of the particle radius and times in units of the Brownian time ($= R^2/6D_0$). Dashed lines of unit slope indicate diffusive limits. The inset shows the corresponding ISFs.

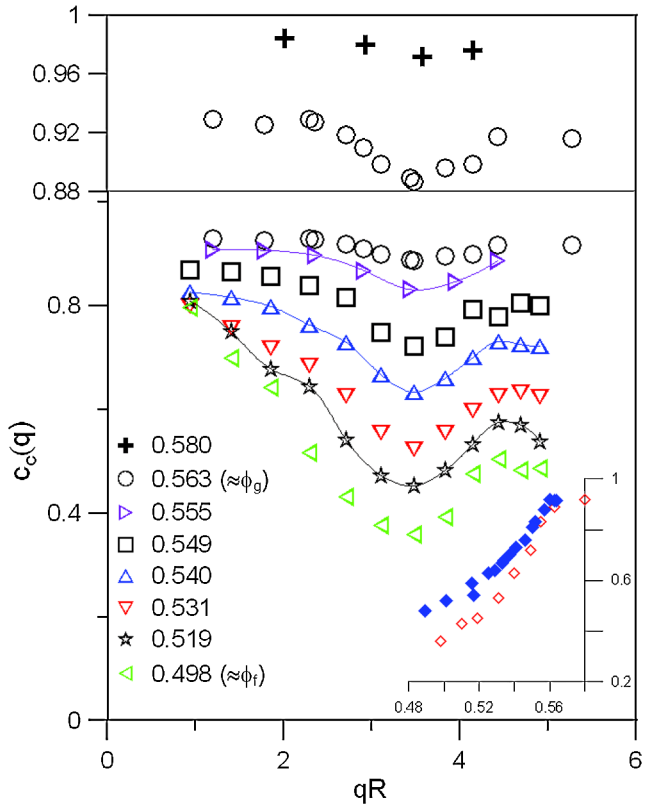

FIG. 2 (color online). Stretching indices [defined in Eq. (3)] versus wave vector for the volume fractions indicated. The scale of the top panel is 4 times that of the bottom panel. The data for $\phi = 0.58$ are for an "aged" sample (see Ref. [18]). Lines drawn on alternate data sets are guides to the eye. The inset shows $c_c(q_m)$ (open diamonds) and c_s (filled diamonds) for all experimental volume fractions.

[Eq. (3)]. Accordingly, we read in c_s [or $c_c(q)$] the correlation of forward and backward displacements, due to packing constraints, of those particles still contributing to the fluctuations at delay time $\tau_m^{(s)}$ [or $\tau_m^{(c)}(q)$]. So, for a suspension in the limit of infinite dilution, where all particles engage in random Markovian excursions, $c_s = c_c(q) = 0$, and the delay times $\tau_m^{(s)}$ and $\tau_m^{(c)}(q)$ are undefined. Approaching the perfect glass, where no particle percolates the system, c_s and $c_c(q)$ approach one and $\tau_m^{(s)}$ and $\tau_m^{(c)}(q)$ become infinite. Between these idealizations, $\tau_m^{(s)}$ and $\tau_m^{(c)}(q)$ are the delay times that must be exceeded for tagged particle motion and number density fluctuations of spatial frequency q, respectively, to forget the effects of packing constraints.

Figures 2 and 3 show $c_c(q)$ and $\tau_m^{(c)}(q)$, respectively. The variation with q of both $c_c(q)$ and $\tau_m^{(c)}(q)$ decreases with increasing ϕ. Though $c_c(q)$ retains some q dependence, $\tau_m^{(c)}(q)$ shows no systematic variation with q at ϕ_g. Of course, given the stretching of $w(q, \tau)$, it suffers more uncertainty than $c_c(q)$. Nonetheless, for a given q, one generally sees that both $\tau_m^{(c)}(q)$ and $c_c(q)$ increase with volume fraction: As expected, density fluctuations become slower and more strongly non-Fickian as ϕ increases. Where discernible, minima in $\tau_m^{(c)}(q)$ and $c_c(q)$ indicate that non-Fickian processes are fastest and least subject to packing constraints around q_m. So, while the nonergodicity factor—the contribution of caged particles—is a maximum at q_m [9], the contribution of those (remaining) mobile particles least impeded by packing effects is also exposed at q_m.

Using previous measurements of the MSD [3,4] we compare (i) $c_c(q_m)$ with c_s, the value of the non-Fickian index of the MSD (inset in Fig. 2), and (ii) $\tau_m^{(c)}(q_m)$ with $\tau_m^{(s)}$, the delay time where the MSD shows its greatest stretching (inset in Fig. 3). Note that c_s converges to $c_c(q_m)$ as ϕ approaches ϕ_g and, within experimental error, $\tau_m^{(s)}$ coincides with the minimum value $\tau_m^{(c)}(q_m)$ of $\tau_m^{(c)}(q)$.

From Refs. [3,4], we obtain the MSDs at the volume fractions closest to those of the coherent ISF measurements. Then for each value of $\tau_m^{(c)}(q)$, where the coherent ISF has its maximum stretching, we read the MSD $\langle \Delta r^2[\tau_m^{(c)}(q)] \rangle$ at that delay time. This quantity is shown in Fig. 4. To interpret this, recall that $\tau_m^{(c)}(q)$ is the delay time that must be exceeded for density fluctuations of wave vector q to forget the effects of packing constraints. Thus, $\langle \Delta r^2[\tau_m^{(c)}(q)] \rangle$ is the mean-squared distance particles must traverse for this loss of memory to occur. [To avoid con-

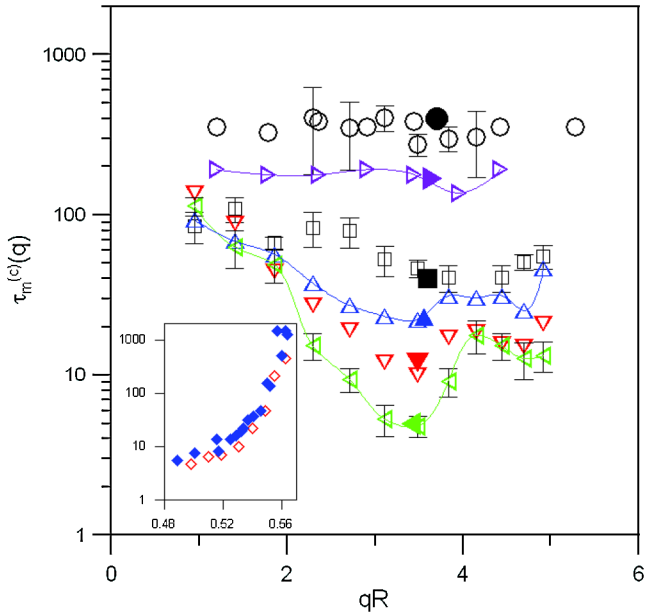

FIG. 3 (color online). Characteristic delay times for selected volume fractions indicated in Fig. 2. Error bars are shown on some data sets. For each data set, the filled symbol indicates the corresponding location of the main structure factor maximum. The inset shows $\tau_m^{(c)}(q_m)$ (open diamonds) and $\tau_m^{(s)}$ (filled symbols) for all experimental volume fractions.

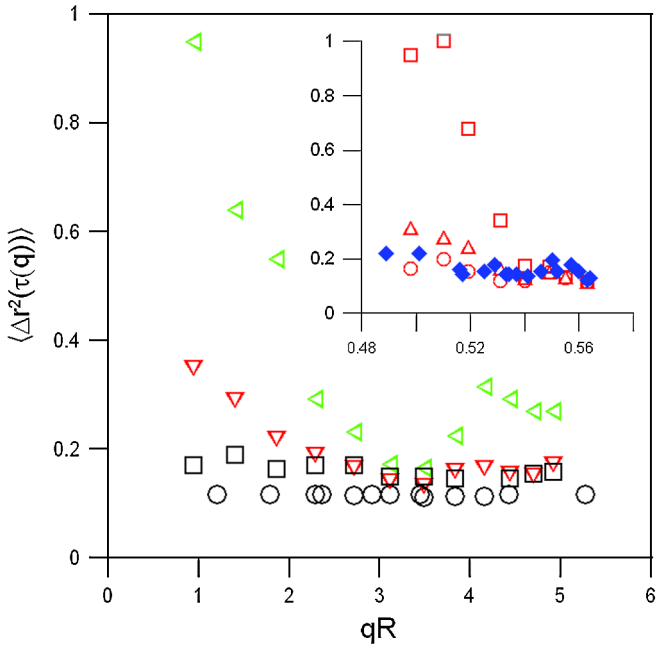

FIG. 4 (color online). MSDs at delay times $\tau_m^{(c)}(q)$ versus the wave vector for selected volume fractions indicated in Fig. 2. The inset shows MSDs at $\tau_m^{(c)}(qR = 1.5)$ (squares), $\tau_m^{(c)}(qR = 3.5 \approx q_m R)$ (circles), $\tau_m^{(c)}(qR = 4.5)$ (triangles), and $\tau_m^{(s)}$ (filled diamonds) for all experimental volume fractions.

fusion in this unconventional analysis, we emphasize that the q dependence of the MSD $\langle \Delta r^2[\tau_m^{(c)}(q)] \rangle$ enters implicitly through the q dependence of the delay time $\tau_m^{(c)}(q)$.] That these MSDs $\langle \Delta r^2[\tau_m^{(c)}(q_m)] \rangle \approx 0.15$ are smallest at q_m is consistent with the q dependence of $\tau_m^{(c)}(q)$ seen in Fig. 3. As also anticipated from the behavior of $\tau_m^{(c)}(q)$, but striking nonetheless, $\langle \Delta r^2[\tau_m^{(c)}(q)] \rangle$ loses its dependence on q with increasing ϕ.

As shown in previous work [10] and shown in Fig. 4 (inset), the value of the MSD at the delay time $\tau_m^{(s)}$ of its maximum stretching shows essentially no systematic variation over the range of volume fractions considered. Since $\tau_m^{(c)}(q_m) \approx \tau_m^{(s)}$ (Fig. 3, inset), $\langle \Delta r^2[\tau_m^{(c)}(q_m)] \rangle$ ($\approx$0.15) displays the same lack of sensitivity to the volume fraction. This saturation of the MSD hints at an interruption in the decay of density fluctuations of spatial frequency q_m due, presumably, to some structural impediment. As far as we can gauge, this interruption, or pause, sets in around the freezing volume fraction ϕ_f (see also Fig. 4 of Ref. [10]). Then as ϕ increases it is seen to spread to other wave vectors from q_m in both directions. In particular, large scale displacements, generally exposed at lower q, decrease most as ϕ approaches ϕ_g. It appears that at ϕ_g number density fluctuations, at least within the measured range of spatial frequencies $1 < qR < 5$, all saturate at the same MSD $\langle \Delta r^2[\tau_m^{(c)}(q)] \rangle \approx 0.15$.

Where structural relaxation is interrupted, there will be a corresponding interruption to the system's ability to respond to diffusing momentum currents, i.e., viscous flow. The local violation of momentum conservation, implied here, is also evident from an absence of or incompatibility with the classical $\tau^{-3/2}$ hydrodynamic "tail" in the velocity autocorrelation function (VAF), for both colloidal [10,11] and Newtonian [12] hard-sphere systems. These studies show, more definitively, that this dynamical anomaly sets in at ϕ_f. They also show that the structural impediment, whose morphology has been associated with the dynamical heterogeneity implicit in the above distinction between caged and mobile particles, is an intrinsic feature of the undercooled hard-sphere system [11,12]. In other words, dynamical heterogeneity—clusters, within which particles are immobilized, immersed in relatively more mobile material—exposed in microscopic experiments [13] and often used to characterize collective processes in undercooled fluids [14] should be considered perhaps in the context of the first-order transition.

So long as the diffusing momentum is blocked by spatial modes in the range $q_m \pm \delta q$, say, it can still "leak" through those spatial modes outside this range. So the final decay [for $\tau > \tau_m^{(c)}(q)$] of density fluctuations in the said range of spatial modes, that no longer couple directly to the diffusing momentum, is delayed by the decay of those that do. Although the suspension still flows, the presence of these structural impediment prevents the (Newtonian) viscosity in the limit of zero shear rate from being attained. This inference is consistent with that based

on the VAF [11], as well as measurements of the rheology [15] of hard-sphere suspensions.

From the apparent divergences of $\tau_m^{(c)}(q_m)$ and $\tau_m^{(s)}$, seen in Fig. 3 (inset) as ϕ approaches ϕ_g, one anticipates, in response to the potential blocking of all spatial modes to momentum diffusion, complete cessation of flow. This would signal the transition to the perfect glass—a sharp ergodic to nonergodic transition, as predicted by the idealized mode coupling theory (MCT) [16]. This theory's predictions describe quantitatively both the coherent [2] and incoherent [17] ISFs measured for these suspensions in many significant respects. However, as shown in Ref. [18], colloidal glasses age. The mere fact that they do so is one indication that there is a mechanism we have not considered—the effect of the thermal energy left undissipated by the above structural impediment to momentum diffusion. As proposed above, this emerges at ϕ_f. Then as ϕ is increased, and the spread of spatial modes closed to viscous flow increases, one reaches a crossover where stationary processes have become so slow that the (final) decay of the ISF, observed in the experimental time window, is effected through nonstationary (aging) rather than stationary processes. In these suspensions, this crossover occurs fairly consistently at, or over a narrow range around, $\phi_g \approx 0.57$.

Moreover, were the colloidal glass perfect, one would expect $c_c(q)$ and c_s to equal one. One sees from the top panel of Fig. 2 that this is not the case. Presumably then, the differences of $c_c(q)$ from one are indicative of those, ergodicity restoring, processes omitted by the idealized MCT. Accordingly, we read in these differences a manifestation of the undissipated thermal energy. Now the q dependence of $c_c(q)$ indicates that the efficacy of these processes is strongest around q_m. The system attempts to restore ergodicity through those (local) rearrangements that must ultimately lead to structures that support lattice modes.

To see how the development of the requisite lattice planes can be frustrated so easily by a modest polydispersity (approximately 6%), we consider results from light scattering studies of crystallization of these suspensions [7]. These reveal, more directly than the DLS experiments, the presence of amorphous clusters of particles. They also show that the clusters are embryonic to crystal nuclei. The clusters' average linear dimension, of some 15 particle diameters, shows little variation with either ϕ or polydispersity [7], even though both aspects have a very strong bearing on the time that elapses between the quench and the appearance of Bragg reflections. Of particular significance is the clusters' compactness; for example, the volume fraction within them is approximately 0.61 at the suspension's GT ($\phi \approx 0.565$). So, even a small spread in particle radii, say, a few percent of the mean, would incur, by the requirement of local fractionation, a significant kinetic impediment to the formation of lattice planes [19]. Accordingly, this local compactness can only impede the local rearrangements that the unrelaxed momenta seek to effect. This addresses the second question posed in the opening paragraph of this Letter.

In conclusion, we offer the following response to the first question: As the suspension's volume fraction is increased from ϕ_f, partial arrest of number density fluctuations spreads from the position of the main structure factor peak to other wave vectors. Concomitantly, the resistance to flow increases not just because density fluctuations become slower, as for a system in thermodynamic equilibrium, but also because of a decrease in the number of spatial modes by which thermal energy can dissipate. The thermal energy left undissipated drives activated processes that, inexorably and irreversibly, lead to separation of the (equilibrium) crystal phase. Neglecting the undissipated thermal energy would, in theory, allow density fluctuations of *all* wave vectors to be arrested and flow to cease completely.

[1] P. G. Debenedetti and F. H. Stillinger, Nature (London) **410**, 259 (2001).
[2] W. van Megen and S. M. Underwood, Phys. Rev. E **49**, 4206 (1994).
[3] W. van Megen, T. C. Mortensen, S. R. Williams, and J. Müller, Phys. Rev. E **58**, 6073 (1998).
[4] W. van Megen, T. C. Mortensen, and G. Bryant, Phys. Rev. E **72**, 031402 (2005).
[5] P. N. Pusey and W. van Megen, Nature (London) **320**, 340 (1986).
[6] S. I. Henderson and W. van Megen, Phys. Rev. Lett. **80**, 877 (1998).
[7] H. J. Schöpe, G. Bryant, and W. van Megen, Phys. Rev. Lett. **96**, 175701 (2006); H. J. Schöpe, G. Bryant, and W. van Megen, J. Chem. Phys. **127**, 084505 (2007).
[8] S. M. Underwood and W. van Megen, Colloid Polym. Sci. **274**, 1072 (1996).
[9] W. van Megen, S. M. Underwood, and P. N. Pusey, Phys. Rev. Lett. **67**, 1586 (1991).
[10] W. van Megen and G. Bryant, Phys. Rev. E **76**, 021402 (2007).
[11] W. van Megen, Phys. Rev. E **73**, 020503(R) (2006).
[12] S. R. Williams, G. Bryant, I. K. Snook, and W. van Megen, Phys. Rev. Lett. **96**, 087801 (2006).
[13] A. Kasper, E. Bartsch, and H. Sillescu, Langmuir **14**, 5004 (1998); W. Kegel and A. van Blaaderen, Science **287**, 290 (2000); A. S. Keys *et al.*, Nature Phys. **3**, 260 (2007).
[14] D. Chandler, *et al.*, Phys. Rev. E **74**, 051501 (2006); L. Berthier *et al.*, J. Chem. Phys. **126**, 184504 (2007); G. Szamel, Phys. Rev. Lett. **101**, 205701 (2008).
[15] J. Mewis *et al.*, AIChE J. **35**, 415 (1989).
[16] W. Götze, *Complex Dynamics of Glass Forming Liquids: A Mode-Coupling Theory* (Oxford University Press, Oxford, 2009).
[17] W. van Megen, Phys. Rev. E **76**, 061401 (2007).
[18] V. A. Martinez, G. Bryant, and W. van Megen, Phys. Rev. Lett. **101**, 135702 (2008).
[19] S. R. Williams, I. K. Snook, and W. van Megen, Phys. Rev. E **64** 021506 (2001); S. R. Williams, C. P. Royall, and G. Bryant, Phys. Rev. Lett. **100**, 225502 (2008).